View Article Online / Journal Homepage / Table of Contents for this issue



# Electrochemical biosensors based on redox carbon nanotubes prepared by noncovalent functionalization with 1,10-phenanthroline-5,6-dione

**Xuyan Mao, Yanhui Wu, Lanlan Xu, Xiaojuan Cao, Xiujun Cui and Liande Zhu***

*Received 12th June 2010, Accepted 17th September 2010*
**DOI: 10.1039/c0an00402b**

Published on 19 October 2010. Downloaded by University of California - Irvine on 29/10/2014 22:01:32.

To improve the electrocatalytic activities of carbon nanotubes (CNT) towards the oxidation of nicotinamide adenine dinucleotide (NADH), we derive them with a redox mediator, 1,10-phenanthroline-5,6-dione (PD), by the noncovalent functionalization method. The redox carbon nanotubes (PD/CNT/GC) show excellent electrocatalytic activities towards the oxidation of NADH (catalytic reaction rate constant, $k_h = 7.26 \times 10^3$ $M^{-1}$ $s^{-1}$), so the determination of NADH can be achieved with a high sensitivity of 8.77 μA $mM^{-1}$ under the potential of 0.0 V with minimal interference. We also develop an amperometric ethanol biosensor by integration of alcohol dehydrogenase (ADH) within the redox carbon nanotubes (PD/CNT/GC). The ethanol biosensor exhibits a wide linear range up to 7 mM with a lower detection limit of 0.30 mM as well as a high sensitivity of 10.85 nA $mM^{-1}$.

## Introduction

Because dihydronicotinamide adenine dinucleotide (NADH) and its oxidized form ($NAD^+$) are cofactors of hundreds of dehydrogenase enzymes, the electrochemical oxidation of NADH is of great interest in the construction of electrochemical biosensors in which the efficient recycling of NADH/$NAD^+$ is necessary.[1,2] The key issue associated with the direct oxidation of NADH is that the reaction is highly irreversible at conventional solid electrodes and only takes place at considerable overpotentials owing to the sluggish charge transfer (*e.g.* 1.1 V and 1.3 V at carbon[3] and Pt,[4] respectively), which leads to serious interference from the concomitant electroactive species, such as ascorbic acid, acetaminophen and uric acid. High overpotential also favors the formation of some inactive dimers that contaminate the electrode surface (electrode fouling).[5] To resolve the problems, the exploitation of new forms of carbon based electrode, *e.g.* carbon nanotubes (CNT),[6,7] graphene,[8] and ordered mesoporous carbon,[9] has become a popular trend. Among those carbon materials, CNT have received particular attention owing to their unique chemical, electronic and mechanical properties.[10,11] Unfortunately, the overpotential decrements for NADH oxidation at CNT were greatly varied among literature reports. For example, Musameh *et al.* reported that the oxidation peak potentials of NADH ($E_p$) were lowered to 0.33 V and 0.36 V at single- and multi-walled carbon nanotube electrodes.[12] Chen and Cai observed that the $E_p$ was close to 0.04 V at the ordered carbon nanotube electrodes.[13] Gong *et al.* reported that the $E_p$ was shifted from 0.60 V to 0.15 V at the vertically aligned CNT which were electrochemically pretreated at 1.8 V for 3 min in pH 6.5 phosphate buffer solution.[14] Yet another study concluded that the electrooxidation of CNT at 1.75 V for 3 min in pH 7.4 phosphate buffer solution had no effect on the oxidation potential.[15] Wooten and Gorski[6] reported that the anodic peak potential of NADH was shifted from 0.4 V to 0 V at treated CNT (boiling in water). The inconsistency of the oxidation potentials demonstrates that the electrochemical activities of CNT are strongly dependent on the synthetic and pretreatment approaches, which would produce different densities of oxygen-related functional groups responsible for catalytic performances, *e.g.* quinone groups.[16,17] Another problem encountered was that CNT also display remarkable catalytic properties towards the oxidation of some other biological substances such as ascorbate, acetaminophen, dopamine, urate, *etc.*,[18] which profoundly overshadows the specificity of CNT to NADH and makes it difficult to selectively determine NADH in the presence of those compounds.

CNT are composed of seamlessly rolled up graphene sheets and therefore exhibit a special sidewall curvature, and possess a π-conjugated structure with a highly hydrophobic surface. These unique properties of CNT essentially allow versatility to be non-covalently functionalized with some organic compounds, in particularly aromatic compounds, through the π–π electronic and hydrophobic interactions without destroying their electronic and chemical structures.[19–23] Therefore, it is rational to derivatize CNT with quinoid compounds by this method to introduce a much greater density of functional groups responsible for facilitating the oxidation of NADH. In this work, multiwalled carbon nanotubes (CNT) were functionalized with a kind of heterocyclic *o*-quinone, 1,10-phenanthroline-5,6-dione (PD) by this method to endow CNT with redox properties that could efficiently accelerate the oxidation speed of NADH. The redox carbon nanotubes were also employed as bioplatforms where alcohol dehydrogenase (ADH) was anchored for the fabrication of ethanol biosensors. Before this time, PD was seldom used as the redox mediator for the oxidation of NADH due to its irreversible electrochemical behavior in weak acidic and basic media. The reduced form is prone to precipitation from the solution and thus eliminates the observation of the reoxidation current. Therefore, 1,10-phenanthroline-5,6-dione transition metal complexes have been frequently adopted for the oxidation of NADH and fabrication of ethanol biosensors previously.[24–26]

*School of Chemistry, Northeast Normal University, Changchun, 130024, Jilin, China. E-mail: zhuld108@nenu.edu.cn; Fax: +86-431-85269667; Tel: +86-431-85099787*

View Article Online

Published on 19 October 2010. Downloaded by University of California - Irvine on 29/10/2014 22:01:32.

## Experimental section

### Reagents

1,10-Phenanthroline-5,6-dione (PD), alcohol dehydrogenase (ADH, EC 232.870.4, 451 U $mg^{-1}$, from Bakers Yeast), ascorbic acid (AA), acetaminophen (AP), dopamine (DA), uric acid (UA), β-nicotinamide adenine dinucleotide, reduced disodium salt hydrate (NADH) and Nafion (5% in alcohol) were obtained from Sigma-Aldrich. Multi-walled carbon nanotubes (CNT, diameter: 20–50 nm, average length: 1–2 μm, purity: ≥95%, surface area: 40–300 $m^2$ $g^{-1}$, amorphous carbon: ≤3%) were purchased from Shenzhen Nanotech. Port. (Shenzhen, China). The as-received CNT were further purified by refluxing in concentrated nitric acid for 48 h to eliminate amorphous carbon and metal oxide catalysts, then washed until the pH of the filtrate approached 7 and finally dried at 50 °C in vacuum. Then the treated CNT were dispersed in *N*,*N*-dimethylformamide (DMF) with the aid of ultrasonic agitation to yield a homogenous dark black suspension (1 mg $mL^{-1}$). All other chemicals were analytical grade and used as received. Aqueous solutions were prepared with doubly distilled water.

### Instrumentation

Electrochemical measurements were performed with a CHI 660B electrochemical workstation (Chenhua Instruments Co., Shanghai, China). The electrochemical cell was assembled with a conventional three-electrode system. A coiled platinum wire was used as a counter electrode. A redox carbon nanotube-coated glassy carbon (GC) was used as the working electrode. All potentials are referenced to a sodium saturated calomel electrode (SSCE). The cell was a one compartment cell with an internal volume of 10 mL. The three electrodes were inserted into the cell through holes in its Teflon cover.

### Procedures

**Preparation of PD/CNT/GC electrode.** A glassy carbon (GC, 3 mm in diameter, CHI 104) electrode was carefully polished with 1.0, 0.3 and 0.05 μm alumina slurries, respectively, and rinsed thoroughly with doubly distilled water between each polishing step, then washed successively with 1 : 1 nitric acid, acetone, and doubly distilled water in an ultrasonic bath, and finally dried in air. Subsequently, 5 μL of the CNT suspension (1 mg $mL^{-1}$ in DMF) was cast onto the surface of the pretreated GC electrode with a microsyringe and the solvent was allowed to dry under an infrared lamp for 30 min. A PD derived redox carbon nanotube-modified electrode (denoted by PD/CNT/GC) was prepared by immersing the CNT coated GC electrode in 1 mM PD solution (in ethanol) for 5 min. Then, PD could be firmly adsorbed on the surface of the CNT/GC electrode. The prepared electrode was washed with copious amounts of distilled water and then dried at ambient temperature before use. PD adsorbed on GC electrode (denoted by PD/GC electrode) was also prepared in the same way just for comparison when necessary.

**Preparation of ethanol biosensor.** 100 μL 0.5% (wt.%) Nafion solution diluted by phosphate buffer solution (pH 6.85) was mixed with 1 mg ADH to give a homogenous ADH/Nafion mixture. Then, 5 μL (containing ~22 U ADH) of the resulting mixture was coated onto PD/CNT/GC electrode. The prepared electrode was dried at room temperature for 15 min and stored at 4 °C when not in use.

## Results and discussion

### Voltammetric behaviors of the PD/CNT/GC electrode

Fig. 1 depicts the cyclic voltammetric (CV) responses of the PD/CNT/GC (a) and PD/GC (b) electrodes in pH 6.85 phosphate buffer solution recorded at a scan rate of 50 mV $s^{-1}$. Both curves show a couple of well-defined peak waves in connection with the redox transformation of the adsorbed PD molecules. Though the shapes are quite different, the anodic and cathodic peak currents (abbreviated as $I_{pa}$ and $I_{pc}$, respectively) are practically identical in both cases, suggesting the redox reactions of PD on GC and CNT are essentially reversible. In contrast, the PD/CNT/GC displays better electrochemical responses in terms of peak current ($I_p$) and peak separation ($\Delta E_p$). The peak currents of PD/CNT/GC are much larger than those of PD/GC, which is mainly attributed to the three dimensional porous structure of the CNT film, resulting in a higher roughness factor which enhances the quantity of adsorbed PD. $I_p$ is linearly proportional to the scan rate in accordance with the pattern of a surface controlled process. However, the peak separations ($\Delta E_p$) are not zero as theoretically expected by an ideal surface confined redox reaction. For instance, at a scan rate of 50 mV $s^{-1}$, $\Delta E_p$ are about 60 and 100 mV for PD/CNT/GC and PD/GC respectively. Furthermore, as the scan rate accelerates (at higher scan rate), the anodic and cathodic peaks start to move in opposite directions so that the peak separations are enlarged, suggesting the redox processes become quasi-reversible. But the formal potentials ($E^{0\prime}$) are independent of the scan rate, which can be estimated by taking the arithmetic mean of anodic and cathodic peak potentials. The $E^{0\prime}$ of the PD/GC electrode was determined to be around −100 mV in pH 6.85 phosphate buffer, which was identical to that of freely diffusional PD under the same conditions. In the case of the PD/CNT/GC electrode, however, the $E^{0\prime}$

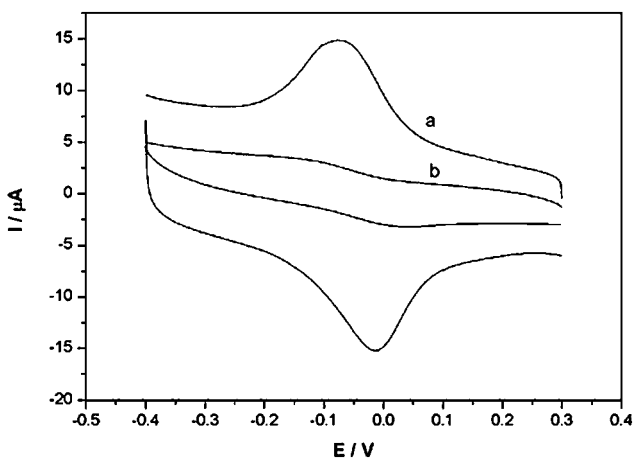


**Fig. 1** Cyclic voltammograms for the PD/CNT/GC (a) and PD/GC (b) electrodes recorded in phosphate buffer solutions (pH 6.85, 0.050 M). Scan rate: 50 mV $s^{-1}$.

 This journal is © The Royal Society of Chemistry 2011

View Article Online

Published on 19 October 2010. Downloaded by University of California - Irvine on 29/10/2014 22:01:32.

was about −53 mV and very close to −60 mV for PD deposited on a pretreated glassy carbon electrode at pH 7.2.[24]

### Kinetic characteristics of the PD/CNT/GC electrode

As stated earlier, the redox reaction of PD/CNT/GC is a surface controlled process. According to Laviron's equation,[27] the relationship between peak current ($I_p$) and surface coverage ($\Gamma$) for a surface process was

$$I_p = \frac{n^2F^2vA\Gamma}{4RT} = \frac{nFQv}{4RT}$$

where $A$ is the surface area (0.0707 $cm^2$ for a flat surface), $Q$ is the total amount of charge, $n$ is the number of electrons transferred, $v$ the scan rate and $F$ is the Faraday constant. From the CV curves, $Q$ was calculated to be $2.17 \times 10^{-6}$ C after background correction. Thus, the average surface concentration ($\Gamma$) of PD was estimated to be about $8.0 \times 10^{-10}$ mol $cm^{-2}$ if a flat surface was assumed.

Fig. 2 (A) shows the magnitudes of the peak potentials ($E_p$) as a function of the logarithm of the potential scan rate. As can be seen in Fig. 2 (B), when the scan rate is above 160 mV $s^{-1}$, $I_p$ becomes linear with the square root of scan rate ($v^{1/2}$). Diffusion of species with fast electrochemical reactions was expected to give a linear relationship between $I_p$ and $v^{1/2}$. At the same time, the wave shapes are distorted severely and the peak separation starts to increase, indicating the electrode reaction becomes electrochemically irreversible at higher scan rates. For an irreversible electrode reaction, the relationship between peak potential and the scan rate follows Laviron's equation.[27]

$$E_{pc} = E^{\circ} + \frac{RT}{\alpha nF}\ln\frac{RTk_s}{\alpha nF} - \frac{RT}{\alpha nF}\ln v \quad (1)$$

$$E_{pa} = E^{\circ} - \frac{RT}{(1-\alpha)nF}\ln\frac{RTk_s}{(1-\alpha)nF} + \frac{RT}{(1-\alpha)nF}\ln v \quad (2)$$

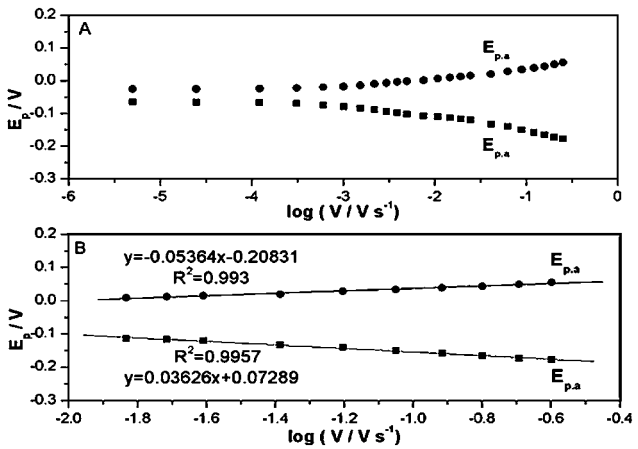


**Fig. 2** (A) Experimental variations of peak potential *vs.* the logarithmic of the scan rate for PD/CNT/GC in phosphate buffer (pH 6.85, 0.050 M). (B) Magnification of the same plots for high scan rates.

$$\Delta E_p = \frac{RT}{(1-\alpha)\alpha nF}[\alpha\ln(1-\alpha) + (1-\alpha)\ln\alpha - \ln\frac{RT}{nF} - \ln k_s] + \frac{RT}{(1-\alpha)\alpha nF}\ln v \quad (3)$$

where $\alpha$ is the electron-transfer coefficient, $k_s$ the standard rate constant of the surface reaction, and $E^{0'}$ the formal potential. $E^{0'}$ (= −0.046 V) could be estimated as the midpoint between the cathodic and the anodic peak potentials at low scan rate. At high scan rate, we can see from Fig. 2 (B), the plots of $E_p$ *versus* ln $v$ are linear:

$$E_{pc} = -0.20831 - 0.05364 \ln v \quad (4)$$

$$E_{pa} = 0.07289 + 0.03626 \ln v \quad (5)$$

From the slope and intercept of the linear curve of $\Delta E_p$–ln $v$, according to eqn (1) and (4), $\alpha n$ was estimated to be 0.471 and $k_s$ to be 0.904 $s^{-1}$ at 25 °C. From eqn (2) and (5), the values of $n(1-\alpha)$, and $k_s$ were obtained as 0.696 and 1.039 $s^{-1}$, respectively. For comparison, the same measurements were also performed with the PD/GC. The $k_s$ values were obtained to be 0.633 and 0.724 $s^{-1}$ for the reduction and oxidation process, respectively, which are lower than those obtained at the PD/CNT/GC. This demonstrates the electron transfer rate of PD/CNT/GC was higher than that of PD/GC.

### Electrocatalytic oxidation of NADH

1,10-Phenanthroline-5,6-dione has been previously shown to be active towards the catalytic oxidation of NADH.[28] In order to test the potential electrocatalytic activities of the redox carbon nanotubes, cyclic voltammetric responses were recorded at PD/CNT/GC and PD/GC electrodes in the absence and presence of NADH. As shown in Fig. 3, upon the addition of 1.0 mM and 5.0 mM NADH, the anodic peak currents increase accompanied by reduced cathodic peak currents in both cases, exhibiting excellent electrocatalytic activities of PD towards the oxidation of NADH. Taking into consideration the results mentioned in the previous section, the behaviors of the PD in the presence of NADH at pH 6.85 could be expressed by the following transformations:

$$PD_{(red)} \leftrightarrow PD_{(ox)} + H^+ + 2e^- \quad (1)$$

$$PD_{(ox)} + NADH \rightarrow PD_{(red)} + NAD^+ \quad (2)$$

Although both the PD/GC and PD/CNT/GC display similar catalytic abilities towards the oxidation of NADH, PD/CNT/GC shows more favorable electrocatalytic activity than PD/GC in terms of onset oxidation potential shapes and peak current. Empirically, the heterogeneous charge transfer rate between NADH and adsorbed PD molecules can be estimated by the ratio of the anodic currents in the presence and absence of the same concentration of NADH. We conclude that the ratio obtained at PD/CNT/GC is much larger than that at PD/GC, indicating the charge transfer rate between NADH and PD/CNT/GC is faster

View Article Online

Published on 19 October 2010. Downloaded by University of California - Irvine on 29/10/2014 22:01:32.

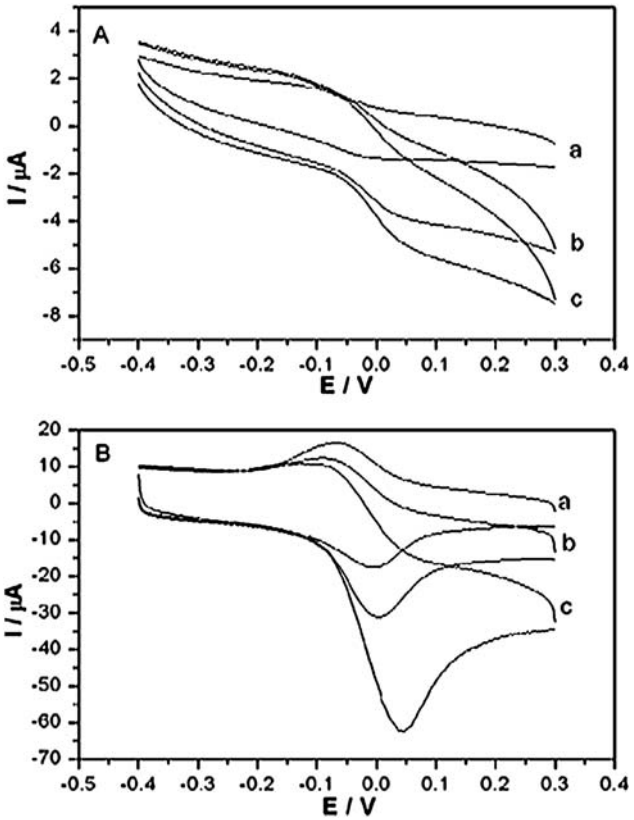


**Fig. 3** Cyclic voltammograms for the PD/GC (A) and PD/CNT/GC (B) recorded in phosphate buffer (pH 6.85, 0.050 M) in the absence (a) and presence of 1.0 mM (b) and 5.0 mM (c) of NADH. Scan rate: 50 mV $s^{-1}$.

than PD/GC. In addition, the fact that the anodic waves achieved at PD/CNT/GC are much sharper than at PD/GC also supports this point.

We further use cyclic voltammetry to semi-empirically determine the catalytic reaction rate constant ($k_h$) between NADH and the adsorbed PD molecules, assuming the charge transfer rate constant between CNTs and the adsorbed PD molecules to be fast. Andrieux and Saveant[29] have analyzed the cyclic voltammograms (CVs) in the framework of a model of redox chemically modified electrodes. Based on extensive computations, a working curve showing the relationship between numerical values of the constant, $I_{cat}/nFAC_b(DnFv/RT)^{1/2}$, and $\log[k_h/(DnFv/RT)^{1/2}]$ (Fig. 1b of Andrieux's article) is given. Here $D$ and $C_b$ are the diffusion coefficient ($cm^2$ $s^{-1}$) and the bulk concentration (mol $cm^{-3}$) of NADH, respectively, and other parameters have their usual meanings. The value of $D$ for NADH has been studied previously,[30] and we chose $3.24 \times 10^{-6}$ $cm^2$ $s^{-1}$ here. The $k_h$ value can thus be calculated from such a working curve. In Fig. 4 (B) we can see the cyclic voltammograms at low scan rates (2–20 mV $s^{-1}$) at the PD/CNT/GC in the presence of 0.40 mM NADH and thus we obtained the average value for the ratio of $I_{cat}/nFAC_b(DnFv/RT)^{1/2}$ to be 0.28 from the average ratio of $I_p/v^{1/2}$ in Fig. 4 (A). Using this value and Fig. 1b of the theoretical paper by Andrieux and Saveant, the value of $k_h$ was determined to be $7.26 \times 10^3$ $M^{-1}$ $s^{-1}$. This value is 1000-fold higher compared to PD/GC (7.50 $M^{-1}$ $s^{-1}$) and close to Re, Fe, and Ru(v-bpy) complexes of PD electrodeposited on a glassy

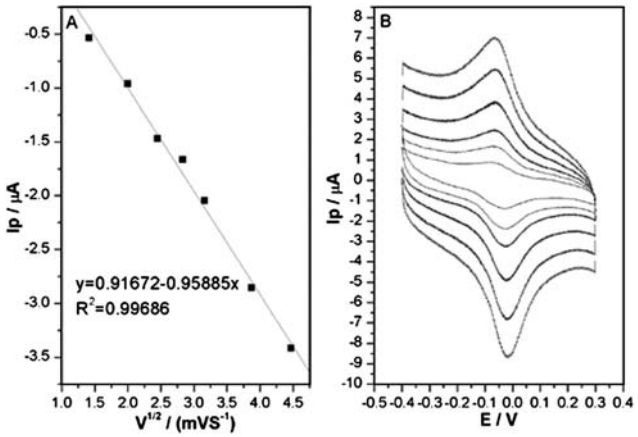


**Fig. 4** (A) Plot of the electrocatalytic currents *vs.* the square root of scan rate derived from data of (B) cyclic voltammograms of PD/CNT/GC in phosphate buffer (pH 6.85, 0.050 M) containing 0.40 mM NADH at different scan rates.

carbon electrode.[24] The value of $k_h$ well illustrates the sharp feature of the catalytic peak observed for catalytic oxidation of NADH at the PD/CNT/GC.

### Amperometric NADH sensor

It was feasible to adopt a relatively lower potential provided by the high efficient catalytic properties of the PD/CNT/GC towards NADH oxidation. The operation potential range of −0.1 to 0 V is regarded as the ideal region for a biosensing system in that most of the electroactive biological substances do not interfere. The interference free behavior of the PD/CNT/GC electrode was illustrated by the amperometric traces performed in a stirred solution, which were spiked with 0.20 mM NADH, 0.10 mM uric acid (UA), 0.10 mM dopamine acid (DA), 0.10 mM acetaminophen (AP) and 0.10 mM ascorbic acid (AA) at three typical operation potentials (0.0, −0.05 and −0.10 V) (see Fig. 5). In all cases, UA, DA and AP showed no obvious interference with NADH. However, under all the operation

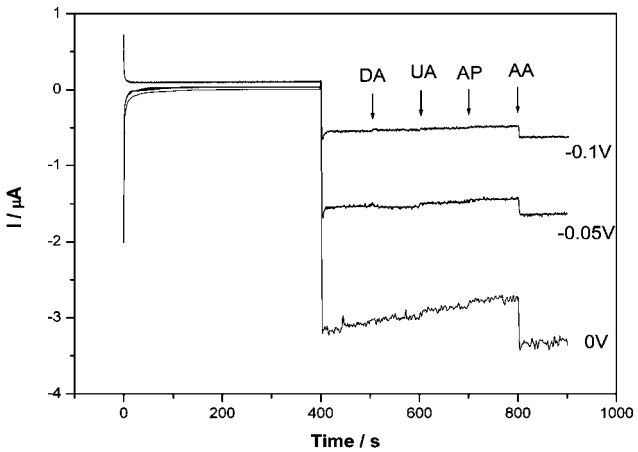


**Fig. 5** Amperometric response of the PD/CNT/GC in phosphate buffer solutions (pH 6.85, 0.050 M) containing 0.20 mM NADH spiked with DA (0.10 mM), UA (0.10 mM), AP (0.10 mM) and AA (0.10 mM).

 This journal is © The Royal Society of Chemistry 2011

View Article Online

Published on 19 October 2010. Downloaded by University of California - Irvine on 29/10/2014 22:01:32.

potentials AA yielded serious anodic current responses. Since the interference brought by AA was inescapable, we set the potential of 0.0 V under which the sensitivity was the highest for the following studies.

Fig. 6 (A) displays the current-time responses of the PD/CNT/GC and the PD/GC electrodes at a working potential of 0.0 V with successive addition of 50 μM NADH into phosphate buffer solution (0.050 M, pH 6.85). The reaction occurring at the PD/CNT/GC was very fast in reaching a dynamic equilibrium upon each addition of the sample solution, generating a steady state current signal within 4 s rather than 10 s at the PD/GC. The linear response of NADH measurement was up to about 500 μM for the PD/CNT/GC, whereas it was only 200 μM for the PD/GC (Fig. 6(B)). The detection limits, based on a signal-to-noise ratio of 3, were estimated to be around 1.8 and 20.2 μM for the PD/CNT/GC and PD/GC electrodes, respectively. From the slope of the calibration curves, much higher sensitivity of 8.77 μA $mM^{-1}$ was obtained for the PD/CNT/GC and it was almost 100 times greater than that of the PD/GC (0.068 μA $mM^{-1}$). Obviously, the amperometric response of the PD/CNT/GC was greatly improved compared with that of the PD/GC.

The reproducibility and stability of the PD/CNT/GC and PD/GC were tested. Eight experiments were carried out in the presence of 1 mM NADH under the operation potential of 0 V. The results demonstrated the PD/CNT/GC had a good reproducibility with a relative standard deviation of 2.2%, while the value for PD/GC was near 4.5%. The storage stability of the modified electrodes was investigated by performing triplicate determination of 1 mM NADH solution in the phosphate buffer daily. When not in use, the sensors were stored at 4 °C in a refrigerator. After 1 month, the PD/CNT/GC still retained about 73% of its original sensitivity, and the response current of the PD/GC based sensor decreased significantly with successive measurements over 15 days.

### Amperometric ethanol biosensor

As discussed above, the redox carbon nanotubes show considerable electrocatalytic properties towards the oxidation of NADH, therefore they may act as bioplatforms for the construction of dehydrogenase based electrochemical biosensors. Herein, we chose alcohol dehydrogenase (ADH) as a model enzyme to illustrate this concept. The ADH was immobilized on the surface of the redox carbon nanotube-modified electrodes (PD/CNT/GC) to develop an ethanol biosensor (ADH/PD/CNT/GC). The quantitation of ethanol in aqueous solution is realized by the amperometric biosensor according to the following schemes: Ethanol is oxidized to acetaldehyde by a coenzyme, nicotinamide adenine dinucleotide (oxidized state, $NAD^+$) which is necessary to accept electrons from ethanol with the aid of ADH. Concurrently, $NAD^+$ is reduced to NADH which can be regenerated and efficiently recycled at the redox carbon nanotube-modified electrode by releasing electrons and a proton.

$$CH_3CH_2OH + NAD^+ \xrightarrow{ADH} CH_3CHO + NADH + H^+ \quad (1)$$

$$NADH \xrightarrow{PD/CNT} NAD^+ + H^+ + 2e^- \quad (2)$$

Thus, the concentration of ethanol can be quantitatively determined by measurement of the anodic current associated with the oxidation of NADH at the redox carbon nanotube-modified electrode.

Fig. 7 displays the amperometric response for successive addition of 1.0 mM ethanol into a stirred phosphate buffer solution (pH 6.85, 0.050 M) containing 2.5 mM $NAD^+$ (A) and the corresponding calibration curve (B) recorded at the ADH/PD/CNT/GC under the operation potential of 0.0 V. Apparently, each addition of ethanol gives rise to a quick steep rise in current above the background which results in a steady state response within 15 s. The linear response range of the biosensor is up to 7.0 mM with a detection limit of 0.30 mM (S/N = 3) and a sensitivity of 10.85 nA $mM^{-1}$. The sensitivity and the steady state response showed good characteristics. The apparent Michaelis–Menten constant ($K_M^{app}$) of the ethanol biosensor was calculated to be 7.25 mM according to the Lineweaver–Burk

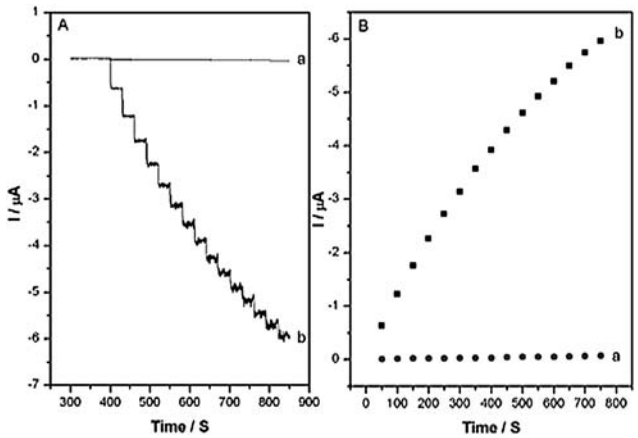


**Fig. 6** (A) Current-time responses for the PD/GC (a) and PD/CNT/GC (b) with successive addition of 50 μM NADH. (B) Calibration curves for NADH at the PD/GC (a) and PD/CNT/GC (b). Operation potential: 0.0 V.

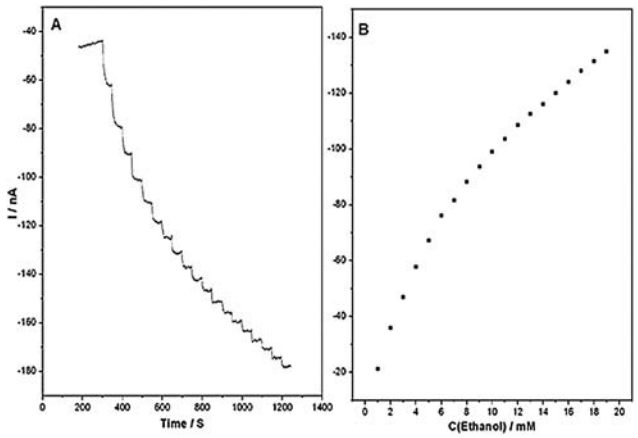


**Fig. 7** (A) Current-time responses for the ADH/PD/CNT/GC with successive addition of 1.0 mM ethanol phosphate buffer (pH 6.85, 0.050 M) containing 2.5 mM $NAD^+$. (B) Calibration curves for ethanol obtained at the ADH/PD/CNT/GC. Operation potential: 0.0 V.

View Article Online

Published on 19 October 2010. Downloaded by University of California - Irvine on 29/10/2014 22:01:32.

equation.[31] This value is similar to that in our previous report (3.15 mM).[32]

The long-term stability (shelf life) of the ethanol biosensor was studied by performing triplicate measurements of 5 mM ethanol solution daily in phosphate buffer. When not in use, it was stored at 4 °C in a phosphate buffer (pH 6.8). The biosensor retained approximately 75.3% of the initial sensitivity after 15 days.

## Conclusions

We demonstrate the concept of redox carbon nanotubes prepared by adsorption of a redox mediator on the surface of carbon nanotubes. The PD-derived redox carbon nanotubes display excellent electrocatalytic activities towards the oxidation of NADH. Based on this experimental fact, we have successfully designed a new NADH sensor with high sensitivity and selectivity. By integration of alcohol dehydrogenase with the redox carbon nanotubes, an amperometric ethanol biosensor has been successfully developed. However, the redox carbon nanotubes also catalyze the oxidation of ascorbic acid, which deteriorates the selectivity of the NADH sensor and the biosensor as well, and needs further investigation.

## Acknowledgements

The authors are profoundly grateful for the financial support from the Training Fund of NENU'S Scientific Innovation Project (No. NENU-STC08011) and the Science Foundation of Jilin Province (20090532).

## References

1 A. Radoi and D. Compagnone, *Bioelectrochemistry*, 2009, **76**, 126.
2 L. Gortona and E. Domınguezb, *Rev. Mol. Biotechnol.*, 2002, **82**, 371.
3 J. Moiroux and P. J. Elving, *Anal. Chem.*, 1978, **50**, 1056.
4 H. Jaegfeldt, *J. Electroanal. Chem.*, 1980, **110**, 295.
5 L. Bartalits, G. Nagy and E. Pungor, *Anal. Lett.*, 1984, **17**, 13.
6 M. Wooten and W. Gorski, *Anal. Chem.*, 2010, **82**, 1299.
7 J. Chen, J. C. Bao and C. X. Cai, *et al.*, *Anal. Chim. Acta*, 2004, **516**, 29.
8 C. N. R. Rao, A. K. Sood and K. S. Subrahmanyam, *et al.*, *Angew. Chem., Int. Ed.*, 2009, **48**, 7752.
9 L. D. Zhu, C. Y. Tian and D. X. Zhu, et al, *Electroanalysis*, 2008, **20**, 1128.
10 A. Lourdes, Y. S. Paloma and J. M. Pingarrón, *Anal. Chim. Acta*, 2008, **622**, 11.
11 J. Wang and Y. Lin, *TrAC, Trends Anal. Chem.*, 2008, **7**, 619.
12 M. Musameh, J. Wang and A. Merkoci, *et al.*, *Electrochem. Commun.*, 2002, **4**, 743.
13 J. Chen and C. X. Cai, *Anal. Chim. Acta*, 2004, **516**, 29.
14 K. Gong, S. Chakrabarti and L. Dai, *Angew. Chem., Int. Ed.*, 2008, **47**, 5446.
15 M. Musameh, N. S. Lawrence and J. Wang, *Electrochem. Commun.*, 2005, **7**, 14.
16 M. Musameh, J. Wang and A. Merkoci, *et al.*, *Electrochem. Commun.*, 2002, **4**, 743.
17 C. N. Rao, B. C. Satishkumar and A. Govindaraj, *et al.*, *ChemPhysChem*, 2001, **2**, 78.
18 L. Agui, P. Y. Sedeno and J. M. Pingarron, *Anal. Chim. Acta*, 2008, **622**, 11.
19 J. Zhang, J. K. Lee and Y. Wu, *Nano Lett.*, 2003, **3**, 403.
20 E. V. Basiuk and E. V. Rybak-Akimova, *Nano Lett.*, 2002, **2**, 1249.
21 A. Star, T. Han and J. P. Gabriel, *Nano Lett.*, 2003, **3**, 1421.
22 Q. Li and J. Zhang, *Carbon*, 2004, **42**, 287.
23 W. Gang, J. P. Chang and J. Reichert, *et al.*, *Carbon*, 2010, **48**, 3.
24 Q. Wu, M. Maskus and F. Pariente, *et al.*, *Anal. Chem.*, 1996, **68**, 3688.
25 G. Hilt, T. Jarbawi, W. R. Heineman and Eberhard Steckhan, *Chem.–Eur. J.*, 1997, **3**, 97.
26 F. Tobalina, F. Pariente, L. Hernández, H. D. Abruña and E. Lorenzo, *Anal. Chim. Acta*, 1999, **395**, 17.
27 E. Laviron, *J. Electroanal. Chem.*, 1974, **52**, 355.
28 S. Itoh, H. Fukushima and M. Komatsu, *et al.*, *Chem. Lett.*, 1992, 1583.
29 C. P. Andrieux and J. M. Saveant, *J. Electroanal. Chem.*, 1978, **93**, 163.
30 H. R. Zare and S. M. Golabi, *J. Solid State Electrochem.*, 2000, **4**, 87.
31 R. A. Kamin and G. S. Wilson, *Anal. Chem.*, 1980, **52**, 1198.
32 X. Y. Jiang, L. D. Zhu and D. X. Yang, *et al.*, *Electroanalysis*, 2009, **21**, 1617.

 This journal is © The Royal Society of Chemistry 2011